High Freestream Turbulence Effects on Turbulent Boundary Layers

K. A. Thole
Assistant Professor,
Mechanical Engineering Department,
University of Wisconsin,
Madison, WI 53706-1572

D. G. Bogard
Associate Professor,
Mechanical Engineering Department,
University of Texas,
Austin, TX 78712-1063

High freestream turbulence levels significantly alter the characteristics of turbulent boundary layers. Numerous studies have been conducted with freestreams having turbulence levels of 7 percent or less, but studies using turbulence levels greater than 10 percent have been essentially limited to the effects on wall shear stress and heat transfer. This paper presents measurements of the boundary layer statistics for the interaction between a turbulent boundary layer and a freestream with turbulence levels ranging from 10 to 20 percent. The boundary layer statistics reported in this paper include mean and rms velocities, velocity correlation coefficients, length scales, and power spectra. Although the freestream turbulent eddies penetrate into the boundary layer at high freestream turbulence levels, as shown through spectra and length scale measurements, the mean velocity profile still exhibits a log-linear region. Direct measurements of total shear stress (turbulent shear stress and viscous shear stress) confirm the validity of the log-law at high freestream turbulence levels. Velocity defects in the outer region of the boundary layer were significantly decreased resulting in negative wake parameters. Fluctuating rms velocities were only affected when the freestream turbulence levels exceeded the levels of the boundary layer generated rms velocities. Length scales and power spectra measurements showed large scale turbulent eddies penetrate to within $y^+ = 15$ of the wall.

Introduction

Highly turbulent freestream effects on boundary layer flows are relevant in such flow geometries as along gas turbine blades, in heat exchangers, and in combustors. It is well-documented that freestream turbulence levels of 7 percent and less, increase skin friction and heat transfer. More recently, studies of increases in skin friction and heat transfer due to high freestream turbulence have been extended to turbulence levels much greater than 10 percent. However, there has been little study of the detailed characteristics for a boundary layer affected by turbulence levels above 10 percent, such as mean and rms levels, correlation coefficients, power spectra, and length scales. This paper presents these detailed characteristics for high freestream turbulence levels ranging between 10 percent < Tu < 20 percent.

There have been numerous studies of freestream turbulence effects on boundary layers, dating back to Kestin (1966), in which grids were used to generate turbulence levels up to 7 percent. The primary objectives of these past studies have been from a practical standpoint of finding parameters to correlate increases of skin friction and surface heat transfer. These increases were generally correlated as a function of turbulence level (Tu) alone. Later, Hancock and Bradshaw (1983) and Blair (1983) showed that increases in skin friction best scaled using a combination of turbulence level and turbulence length scale (L_ϵ^u) in terms of a β parameter defined as,

$$\beta = \frac{\mathrm{Tu}(\%)}{\left(\frac{L_\epsilon^u}{\delta} + 2\right)} \tag{1}$$

Hancock and Bradshaw (1983) and Blair (1983) also showed that as freestream turbulence levels start to increase, the outer regions of the velocity boundary layers exhibited a depressed wake region. At a turbulence level of Tu = 5.3 percent, the wake region was essentially nonexistent.

Both the Hancock and Bradshaw (1983) and Blair (1983) studies, as well as other grid-generated turbulence studies, have presumed that the log-law was valid for a boundary layer influenced by freestream turbulence levels of Tu = 7 percent or less. Hence, the wall shear stress for these studies were obtained from Clauser fits of the near-wall velocity profile. In a later study, Hancock and Bradshaw (1989) measured various terms in the turbulent energy transport equation to determine whether there was local equilibrium between production and dissipation in the near-wall region. Bradshaw (1978) had presented arguments that the log-law holds when there is local equilibrium in the near wall-region. For a freestream turbulence level of 4 percent, Hancock and Bradshaw found that near the wall there was a definite increased loss of turbulent energy by diffusion. Although this loss increased with freestream turbulence, it was still small relative to the production and dissipation terms. Hence, the boundary layer influenced by turbulence levels of 4 percent was found to be in local-equilibrium. Although this energy balance supports the validity of the log-law for the lower turbulence freestream turbulence levels, the question still remains whether the boundary layer stays in equilibrium at turbulence levels above 4 percent.

Conditional sampling studies were included in the Hancock and Bradshaw (1989) freestream turbulence study and were also performed by Charnay, Mathieu, and Comte-Bellot (1976). In these conditional sampling studies, the boundary layer fluid was thermally tagged through the use of a heated test plate. By thermally tagging the boundary layer fluid, a distinction could be made between the turbulence statistics associated with the boundary layer and freestream fluid elements. Hancock and Bradshaw used conditional sampling analyses to study turbulent stress statistics within the hot boundary layer fluid and the cold freestream fluid. Of particular interest was that, for low freestream turbulence, R_{uv} correlation coefficients for the freestream

Contributed by the Fluids Engineering Division for publication in the JOURNAL OF FLUIDS ENGINEERING. Manuscript received by the Fluids Engineering Division December 27, 1994; revised manuscript received January 28, 1996. Associate Technical Editor: F. Giralt.

fluid which penetrates well within the boundary layer are quite large. However, for higher freestream turbulence levels, the R_{uv} correlation coefficients for freestream fluid decreased substantially. Charnay et al. had a significant difference in the way that fluctuating velocity components were defined. Charnay et al. defined the fluctuating components relative to the hot or cold zone average, while Hancock and Bradshaw defined the fluctuating components relative to the total time average. With this difference, Charnay et al. found that the freestream fluid had a relatively low R_{uv} correlation coefficient with similar levels for freestream turbulence levels ranging from Tu = 0.3 to 4.7 percent. Charnay et al. also showed a significant downward zonal mean velocity for the freestream fluid relative to the boundary layer fluid. The magnitude of this relative downward mean velocity increased with increasing turbulence level. Comparing the results of Charnay et al. with those of Hancock and Bradshaw indicates that the high R_{uv} correlation coefficients found by Hancock and Bradshaw was due to a general downward velocity of the freestream fluid penetrating into the boundary layer. The R_{uv} correlation coefficient decreased with increasing turbulence levels because the increased streamwise velocity fluctuations within the freestream fluid were uncorrelated with the general downward movement. These results were important because the general downward movement of the penetrating freestream fluid is identified as a key transport mechanism.

More recently, there have been studies using devices other than grids to generate turbulence levels greater than 7 percent. Ames and Moffat (1990) used a combustor-simulator to generate turbulence levels up to 19 percent, Thole and Bogard (1994) used high-velocity cross jets to generate turbulence levels up to 20 percent, while Maciejewski and Moffat (1989) used a free jet directed over a flat plate to generate turbulence levels up to 60 percent. Both the Ames and Moffat and the Thole and Bogard studies investigated several different parameters, based on freestream turbulence level and length scale, for correlating skin friction and heat transfer.

To date, the interaction between high freestream turbulence levels and turbulent boundary layers for these higher freestream turbulence levels has not been fully investigated. An important issue to be addressed for these types of flows is the validity of the log-law. In addition, there is no data available on how the velocity correlation coefficient (R_{uv}), length scales, and power spectra are affected inside the boundary layer as a result of the highly turbulent freestream. These items are addressed in this paper for freestream turbulence levels ranging between 10 percent < Tu < 20 percent.

Experimental Facilities and Instrumentation

The facility used for the experiments in this paper included a closed-loop, boundary layer wind tunnel in the Turbulence and Turbine Cooling Research Laboratory at the University of Texas at Austin. This section briefly describes the facility, including the turbulence generator, as well as the instrumentation used for these studies.

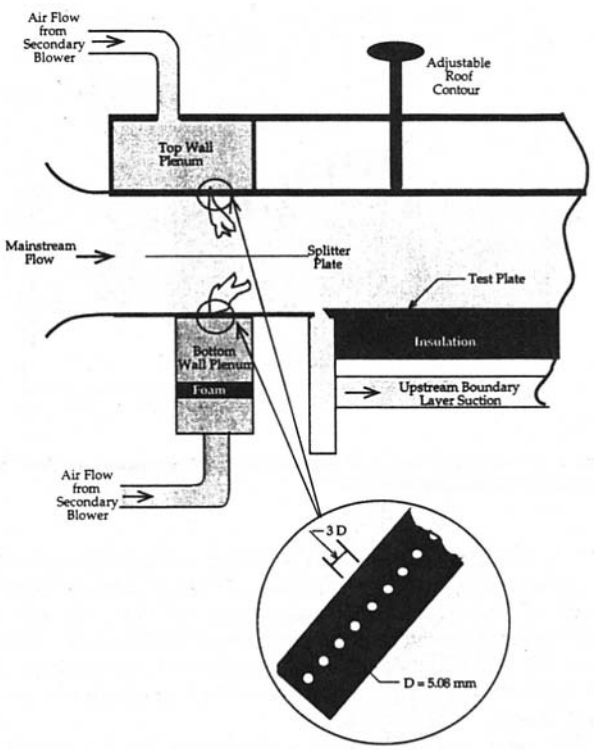

Fig. 1 Schematic of the wind tunnel test section and the turbulence generator

Flow for the closed-loop wind tunnel was driven by a 5-hp fan and adjusted using a frequency-modulated motor controller. Flow conditioning upstream of the test section consisted of a honeycomb section followed by four fine mesh screens. Following these screens was a 9:1 area contraction which was then followed by the test section. Figure 1 is a schematic of the test section which was 244 cm in length, 61 cm in width, and 15.2 cm in height.

As indicated in Fig. 1, the initial 60 cm of the test section was occupied by the turbulence generator. Details of the turbulence generator are presented in Thole, Whan-Tong, and Bogard (1994). The design of the turbulence generator consisted of a row of small, high-velocity, normal jets injecting into the cross-flow mainstream as shown by the inset in Fig. 1. The diameter of the jet holes were 5.08 mm in diameter. The jet holes were spaced three diameters apart and had a length-to-diameter ratio

Nomenclature

D = jet hole diameter
E_u = streamwise velocity power spectral density
f = frequency
L_ϵ^u = dissipation length scale, $L_\epsilon^u = -[(u'^2)^{3/2}/U_\infty(du'^2/dx)]$
Re_D = Reynolds number based on hole diameter
Re_λ = turbulent Reynolds number, $\lambda_g u'/\nu$
Re_θ = Reynolds number based on momentum thickness
R_{uv} = correlation coefficient, $\overline{uv}/u'v'$
Tu = turbulence intensity (%), u'/U_∞
u' = RMS velocity in streamwise direction
u^+ = nondimensional velocity, u/u_τ
u_τ = friction velocity, $\sqrt{\tau_w/\rho}$
U = mean streamwise velocity
U_∞ = mainstream velocity in streamwise direction
$\overline{uv}$ = turbulent shear stress
v' = RMS velocity in normal direction
w' = RMS velocity in the lateral direction
x = streamwise distance
y = vertical distance
y^+ = nondimensional vertical distance, $y \cdot u_\tau/\nu$
β = correlation parameter,
δ = boundary layer thickness, 99 percent point
κ = von Kármán constant
Λ_f = streamwise integral turbulent length scale
θ = momentum thickness
τ_{total} = total shear stress, $(\mu(\partial U/\partial y) - \rho\overline{uv})$
$\tau_{\text{log-law}}$ = wall shear stress determined from the log-law

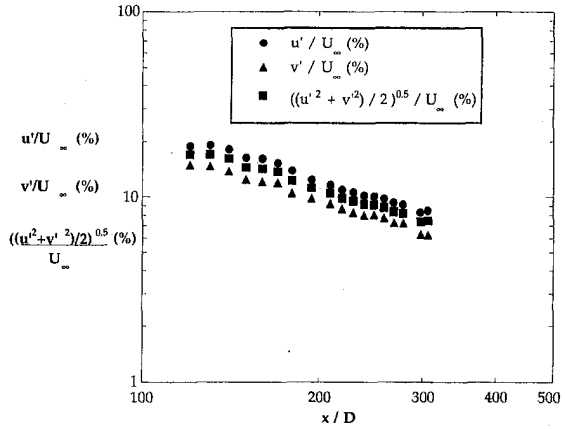

Fig. 2 Streamwise decay of turbulence for streamwise, vertical, and combined fluctuating velocities

of 2.5. The jet holes were located 57.5 hole diameters upstream of the leading edge of the test plate. To achieve the turbulence levels of interest, the jet-to-mainstream velocity ratio was 17, and the jet Reynolds number was $Re_D = 1700$. Mass addition from the normal jets into the mainstream was 20 percent, and the mainstream velocity downstream of the generator was nominally 8 m/s.

The mean and rms velocities as well as the $\overline{uv}$ correlation measurements were made using a Thermal Systems Inc. (TSI) two-component LDV system with frequency shifting. The optical axis of the two component LDV system was inclined slightly to obtain measurements close to the wall. Consequently, v-component measurements were actually inclined at an angle of 10° from the true vertical which caused a bias error of 2 to 6 percent of the v' measurement due to contamination by w' fluctuations. Measurements of simultaneous U and V components of velocity were required to be coincident within a 10 μs window. Incense smoke, filtered to remove inherent tar particles, was used to seed the flow with a particle diameter slightly smaller than 1 μm. The velocity data was corrected for velocity bias errors using residence time weighting (Edwards, 1987). Care was also taken to insure that the large frequency range of the Doppler signal for a highly turbulent flow was measured over a range of flat frequency response for the counter filters.

Integral time scales and power spectra were obtained from hot-wire measurements of the streamwise velocity fluctuations. Power spectra were obtained from a spectrum analyzer. The integral time scales were calculated directly from correlations of the digitized hot-wire measurements, or from the power spectra extrapolated to zero frequency (Hinze, 1975).

Uncertainty Estimates

Precision uncertainties for all measurements were determined statistically using a series of repeatability tests. Mean and rms velocity measurements were made using a sample time of about 60 s. This resulted in precision uncertainties for mean velocities of 1.2 percent in the freestream and 2.3 percent in the near-wall region, and for rms velocities of 1.2 percent in the freestream and 3 percent in the near-wall region. Bias errors for the LDV measurements, including residual errors after velocity bias corrections, uncertainty in fringe spacing, and frequency variations in electronic filtering, resulted in less than 3 percent bias uncertainty for the mean velocity. Uncertainty for the friction velocity, u_τ, was dominated by the uncertainty for the mean velocity measurement which caused a similar 3 percent uncertainty for u_τ. Repeatability tests indicated nominally 5 percent uncertainty for correlation coefficient, R_{uv}, measurements, and nominally 5 percent uncertainty for the integral length scales. For the highly turbulent cases, accurate measurement of the boundary layer thickness δ (based on interpolating the point at which the mean velocity was 99 percent of the freestream) was difficult because of the relatively flat velocity profiles and larger uncertainties for the freestream velocity estimate. The uncertainty of the δ estimate was 2 percent for low freestream turbulence and 10 percent for high freestream turbulence.

Statistics of the Freestream Turbulence Field

Turbulence levels produced by the normal jets-in-crossflow turbulence generator are shown in Fig. 2 as a function of streamwise distance measured from the jet holes. The test plate starts 29 cm downstream from the jet injection ($x/D = 57.5$) with a sharp leading edge. At 8 cm downstream from the start of the leading edge, a 2.4 mm rod was placed to insure a turbulent boundary existed for the low and high freestream turbulence cases. The region of interest for these tests was from 66 cm to 152 cm downstream of the jet injection ($x/D = 130$ to 300). At the $x/D = 130$ location, the mean velocity field was relatively uniform. The turbulence level was Tu = 20 percent at $x/D = 130$ and decayed to a level of Tu = 9 percent at $x/D = 300$. Figure 2 shows both the streamwise and vertical rms velocity components and, as indicated, the turbulent field is slightly non-isotropic. The decay rate for the freestream turbulence compares well with the theoretical decay rate for homogeneous, isotropic turbulence (Hinze, 1975).

The streamwise turbulent integral length scales (Λ_f), the dissipation length scales (L_ϵ^u, defined by Townsend, 1956), and the power spectra for the streamwise velocity fluctuations (E_u) were also documented for this highly turbulent freestream. The integral length scales were deduced from the measured integral time scales and mean velocities invoking Taylor's hypothesis.

Figure 3 shows the streamwise growth of the integral and dissipation scales normalized by the jet hole diameter for the highly turbulent flow field. Both Blair (1983a) and Simonich and Bradshaw (1978) indicated that there was a fixed value for the ratio of dissipation to integral length scales. In these two grid-generated turbulence studies, Blair (1983) reported a ratio of $L_\epsilon^u/\Lambda_f = 1.5$, whereas Simonich and Bradshaw (1978) reported a ratio of $L_\epsilon^u/\Lambda_f = 1.1$. However, Comte-Bellot and Corrsin (1971) show results for grid-generated turbulence indicating a range for this ratio of $1.3 < L_\epsilon^u/\Lambda_f < 1.7$. Also, in the turbulent flowfield generated by a combustor simulator, Ames and Moffat (1990) reported a range of length scale ratios of $1.6 < L_\epsilon^u/\Lambda_f < 2.6$. In the study described here, the dissipation length scales and the integral length scales were similar, as shown in Fig. 3, with a length scale ratio of $1.1 < L_\epsilon^u/\Lambda_f < 1.4$ over the region of interest.

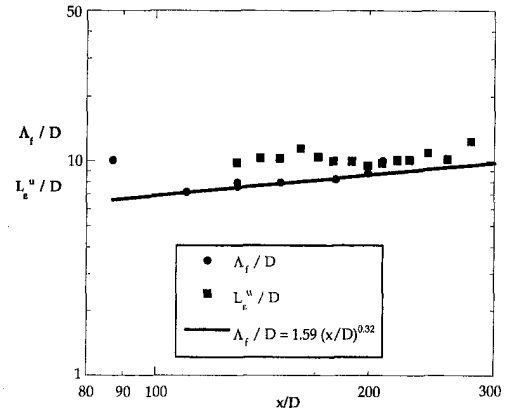

Fig. 3 Streamwise integral and dissipation turbulent length scales for the high turbulent flowfield

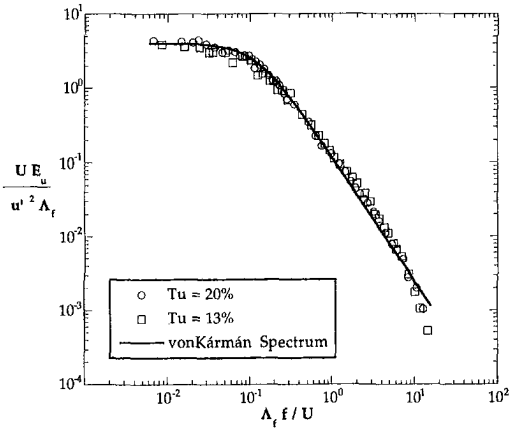

Fig. 4 Energy spectra of freestream turbulence as compared with the von Kármán Spectrum

Of particular importance, in terms of the effect of the freestream turbulence on the boundary layer, was that the ratio of integral length scale to the boundary layer thickness. The integral scale of the freestream turbulence relative to the boundary layer thickness was approximately $\Lambda_f/\delta = 2$ for most of the data analyzed. This ratio of the integral scale to boundary layer thickness was significantly larger than the integral scale of turbulence self-generated in the boundary layer for negligible freestream turbulence (discussed later in this paper). For negligible freestream turbulence, the wall generated turbulence length scale to boundary layer thickness was found to be $\Lambda_f/\delta = 0.4$ through most of the boundary layer.

All high freestream turbulence positions had a nominal Reynolds number of $Re_\theta = 600$, and these data were compared to data from a low freestream turbulence boundary layer which also had $Re_\theta = 600$. For the low freestream turbulence boundary layer, the boundary layer and momentum thicknesses were $\delta = 18$ mm and $\theta = 1.8$ mm, respectively. For the high freestream turbulence conditions, the boundary layer had a constant thickness of nominally $\delta = 20$ mm, and a constant momentum thickness of nominally $\theta = 1.2$ mm along a streamwise distance of 65 cm. With the constant momentum thickness, a momentum integral analysis indicates that a significant pressure gradient exists in the flow. Although the freestream velocity was kept nominally constant, Ames and Moffat (1990) showed that for decaying freestream turbulence levels, similar to that in this study, there was a significant decay in the total pressure of the flow. In fact they found that "acknowledging a total pressure loss along the channel is important in producing a reasonable momentum balance." In a different facility, Sahm and Moffat (1992) found that in a region of decaying high freestream turbulence levels, the boundary layer thickness and momentum thickness actually decreased with streamwise distance.

Figure 4 shows the measured power spectral density in the freestream for turbulence levels of Tu = 20 percent and 13 percent as compared with the classic von Kármán spectrum. These two positions have the maximum and minimum turbulence Reynolds numbers in the flowfield, $Re_\lambda = 271$ and $Re_\lambda = 159$, respectively. The spectra are in good agreement with the von Kármán spectrum and are at a sufficiently high turbulent Reynolds number to have a large inertial subrange.

Effects of Freestream Turbulence on Boundary Layer Mean and RMS Velocities

The wall shear stress for turbulent boundary layer flows is commonly determined by fitting to the mean velocity profile measured near the wall (known as a Clauser fit). The velocity profile is assumed to follow the following log-law profile:

$$U^+ = \frac{1}{\kappa} \ln y^+ + C \qquad (2)$$

where κ is the von Kármán constant, $\kappa = 0.41$, and C is a constant taken to be 5.0. This technique is well established for low freestream turbulence boundary layer flows, and has been assumed to be valid in previous studies with high freestream turbulence. For this study, we were particularly concerned about the applicability of the log-law since freestream turbulence levels were significantly higher than most previous studies. To evaluate the accuracy of the log-law fit for determining wall shear stress, comparisons were made with measurements of the total stress (τ_{total}), i.e. viscous plus turbulent shear stress ($\mu(\partial U/\partial y) - \rho\overline{uv}$), near the wall. The total shear stress data were normalized using wall shear stress determined from a Clauser fit to the log-law, $\tau_{log\text{-}law}$. The Clauser fit was done in the log-law region of the mean velocity profile between $y^+ = 30$ and $y/\delta = 0.2$. Results from these measurements, as shown in Fig. 5, indicate a normalized total stress of nominally $\tau_{total}/\tau_{log\text{-}law} = 1$ near the wall for all freestream turbulence levels, confirming the accuracy of the log-law fit in determining the wall shear stress. Note that a streamwise pressure gradient is expected for this flow due to the decaying freestream turbulence, but this was estimated to have less than a 5 percent effect on the total stress in the near wall region ($y^+ < 50$).

Mean velocity profiles measured in the present study and in previous studies by Johnson and Johnston (1989) and Ames and Moffat (1990) are presented in terms of inner variable scaling in Figure 6a. A distinct log-linear region following the log-law profile is evident for all freestream turbulence levels. This may be explained physically if one assumes that the mean velocity gradient near the wall (in the constant stress region) is proportional to a velocity scale of $(-\overline{uv})^{1/2}$ and the distance from the wall y, i.e., $\partial U/\partial y \sim (-\overline{uv})^{1/2}/y$ (see Gad-el-Hak and Bandyopadhyay, 1994). Integration of this equation results in the well-recognized log-law mean velocity profile. From this viewpoint it is important to recognize that the normalized turbulent shear stress, $-\overline{uv}/u_\tau^2$, is essentially unaffected by the high free-stream turbulence levels in the near wall region as is evident from Fig. 5 where $\tau_{total}/\tau_{log\text{-}law}$ is essentially equal to $-\overline{uv}/u_\tau^2$ (because the viscous stress is negligible). The turbulent shear stress profiles are relatively unaffected by the high freestream turbulence levels in the near wall region because the level of the shear stress in the constant stress layer must be balanced with the wall shear stress, i.e., $-\overline{uv} = u_\tau^2$, regardless of the freestream conditions. Consequently, the mean velocity profile remains unaffected in the log-law region even though the rms turbulence levels significantly increase.

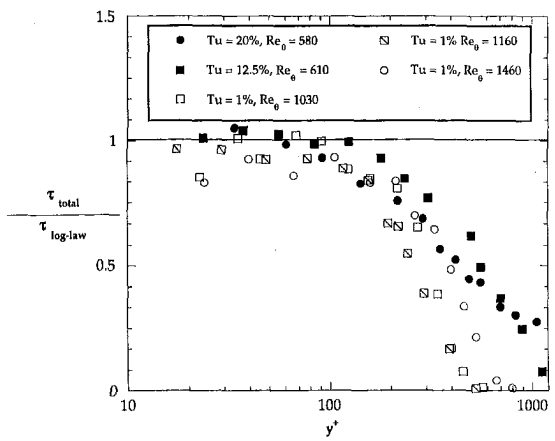

Fig. 5 Total shear stress distribution normalized by the friction velocity obtained from the Clauser fit

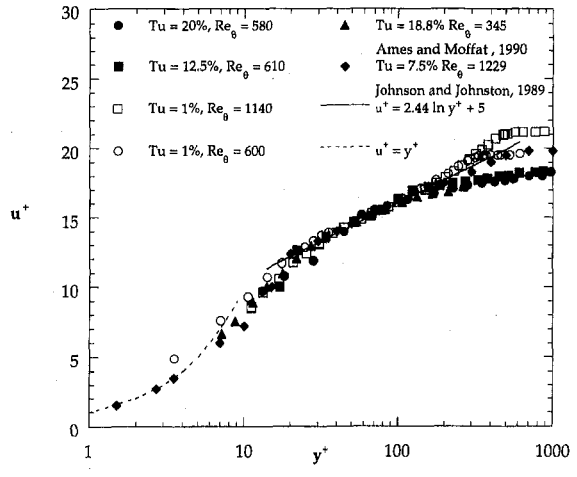

Fig. 6(*a*) Effect of freestream turbulence on the mean velocity in terms of inner variables

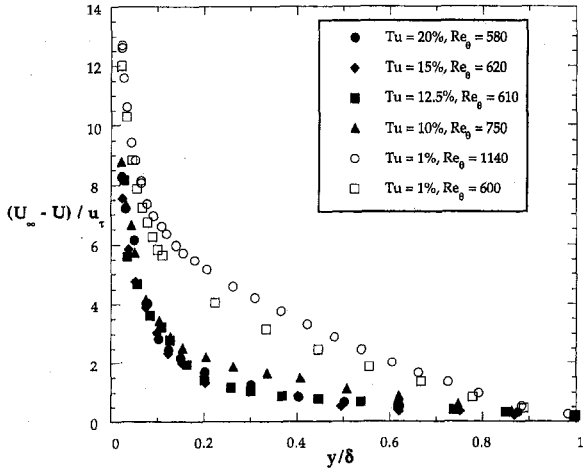

Fig. 6(*b*) Effect of freestream turbulence on the mean velocity in terms of inner variables

Also evident in Fig. 6(a) is a significant alteration of the outer part of the boundary layer due to high freestream turbulence. As the turbulence levels were increased, the mean velocity profiles fell below the log-law resulting in negative wake values. Another perspective of the effect of high freestream turbulence on the outer part of the mean velocity profile is evident from the defect velocity profiles presented in Figure 6(b) with outer scaling for y, i.e., y/δ. Clearly there is distinct difference between the low and high freestream turbulence cases, with much lower defect velocities in the outer region for the high freestream turbulence cases. Note there was a collapse of the defect velocity profiles for freestream turbulence levels above Tu = 12.5 percent which indicates a constant wake strength.

Figure 7 shows the wake parameter, Π, as a function of the Hancock and Bradshaw's β-parameter. The data included in Fig. 7 are results from grid-generated studies such as Johnson and Johnston (1989), Rüd (1985), and Hoffmann and Mohammadi (1991). Also included are higher freestream turbulence measurements of Ames and Moffat (1990) and the present measurements. The wake parameter, Π, was determined using the following relation,

$$\frac{U_\infty}{u_\tau} = \frac{1}{\kappa} \ln \frac{\delta u_\tau}{\nu} + C + \frac{2\Pi}{\kappa} \tag{3}$$

Hoffmann and Mohammadi (1991) showed a systematic decrease in wake strength with increases in β to $\beta = 2$, resulting in a negative wake component for approximately $\beta > 1$. Although there is scatter in the data, at values greater than $\beta = 3$ the data appear to be asymptotically approaching a constant wake strength of $\Pi = -0.5$.

Figures 8(a)–8(d) show the u' and v' velocity profiles plotted in terms of inner variables and outer variables. The rms velocity profiles for the highly turbulent flows are compared with those of a low turbulence (Tu = 1 percent) boundary layer for two different Reynolds numbers. In Figs. 8(a) and 8(b), the data is supplemented with that of Johnson and Johnston (1989) for the turbulence levels of Tu = 7.5 percent (Re_θ = 1230) and Tu < 1 percent (Re_θ = 1450).

Figure 8(a) shows that for turbulence levels less than Tu = 12.5 percent, the u' velocities scale quite well with u_τ in the near-wall region ($y^+ < 40$). However, for higher turbulence levels, Tu > 15 percent, the peak values of u'/u_τ increase ($u'/u_\tau = 3.3$). These profiles indicate the penetration of the freestream turbulence into the boundary layer very close to the wall. For Tu = 15 percent, $u'/u_\tau = 2.8$ throughout most of the boundary layer until very close to the wall where there is a slight increase to $u'/u_\tau = 3.2$. However, for the highest freestream turbulence case, Tu = 20 percent, the streamwise fluctuating velocity is relatively constant across the entire boundary layer with a value of $u'/u_\tau = 3.3$. Ames and Moffat (1990) measured a similar increase in u'/u_τ at high turbulence levels with peak values of $u'/u_\tau = 2.8$ for Tu < 10.5 percent in a Reynolds number range of $875 < Re_\theta < 1179$, and an increase to $u'/u_\tau = 3.4$ for a Tu = 19 percent at a $Re_\theta = 345$.

In Fig. 8(b) the v' profiles are shown to be substantially different from the u' profiles shown in Fig. 8(a). First, scaling of v' with u_τ very near the wall is relatively good for all the turbulence levels. The second noticeable difference is a systematic decrease in v' as the wall is approached. This difference is more clearly seen in comparing Figs. 8(c) and 8(d) where the u' and v' velocity profiles are plotted in terms of outer variables. It is evident that the v' levels are continually decreasing when approaching the wall, whereas the u' profiles are relatively flat (except very near the wall).

The attenuation of v' levels throughout the boundary layer is due to the wall limitation, which is not a restriction for the u' velocity fluctuations. Wall effects on freestream velocity fluctuations were studied analytically by Hunt and Graham (1978) and experimentally by Thomas and Hancock (1978). These studies showed that a wall, which is moving with the flow so that there is no boundary layer, will significantly attenuate the normal velocity fluctuations. Figure 8(e) shows the decrease in v' velocity fluctuations relative to the freestream level as a function of distance from the wall normalized with the integral

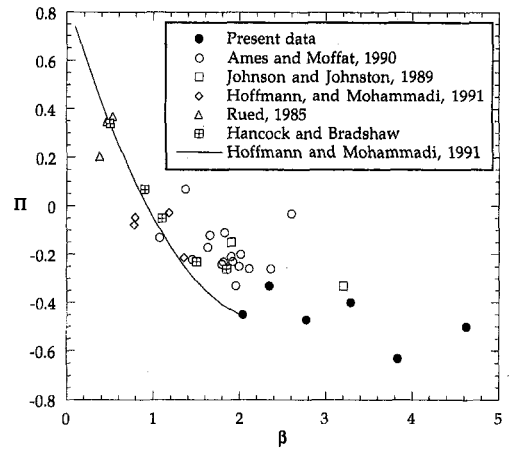

Fig. 7 Wake strengths as a function of the Hancock and Bradshaw's β-parameter

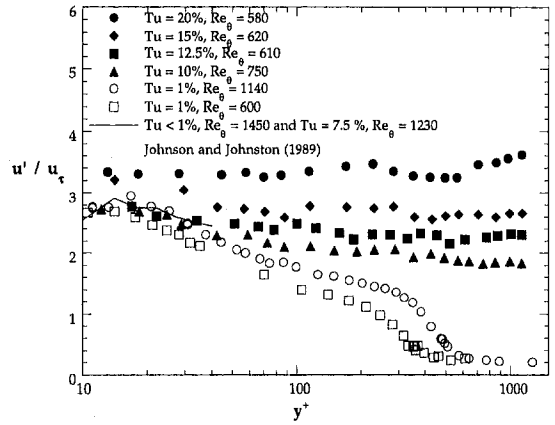

Fig. 8(*a*) Streamwise rms velocity profiles for different turbulence levels plotted using inner variables

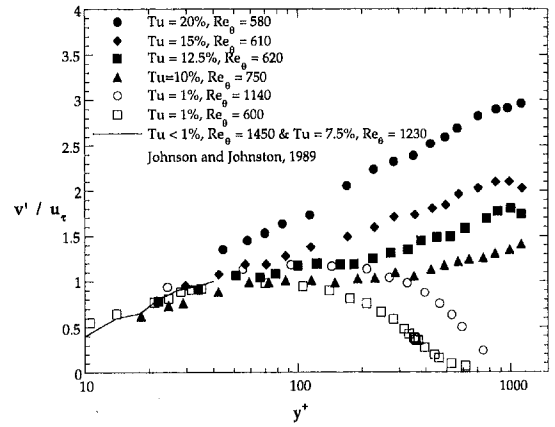

Fig. 8(*b*) Vertical rms velocity profiles for different turbulence levels plotted using inner variables

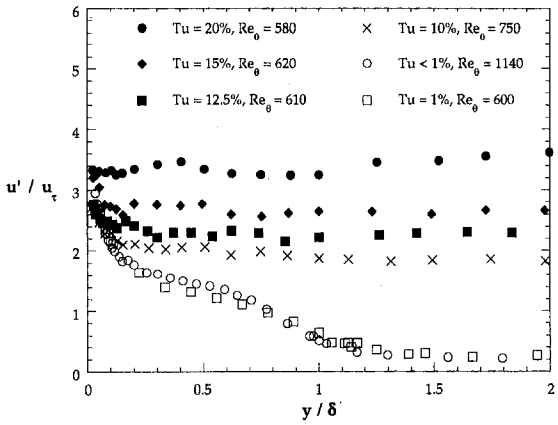

Fig. 8(*c*) Streamwise rms velocity profiles for different turbulence levels in terms of outer variable scaling

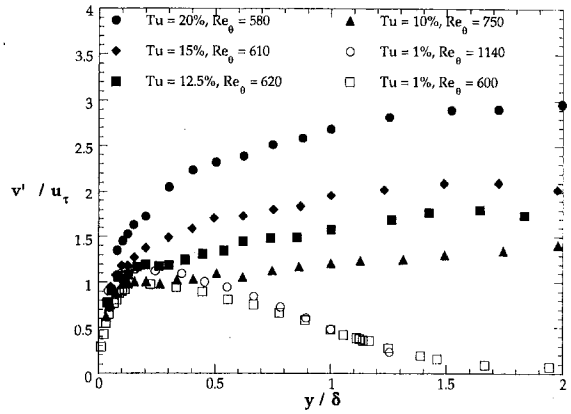

Fig. 8(*d*) Vertical rms velocity profiles for different turbulence levels plotted using outer variables

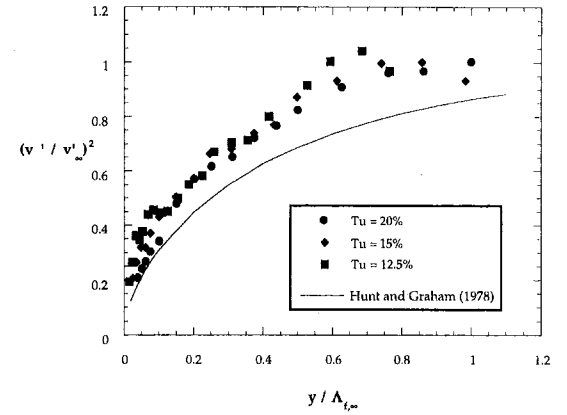

Fig. 8(*e*) Attenuation of the vertical velocity fluctuations as a function of vertical distance normalized by the dissipation length scale (Hunt and Graham, 1978)

length scale of the freestream turbulence. Also shown is the trend predicted by Hunt and Graham. The attenuation of the v' velocity fluctuations was found to be similar to the prediction of Hunt and Graham (also to the measurements of Thomas and Hancock, not shown) suggesting that this attenuation is due to the wall proximity and not caused by the boundary layer flow.

Effects of Freestream Turbulence on Boundary Layer

Power Spectra and Length Scales. The integral length scales as well as the power spectra were measured at several positions throughout the boundary layer. In each case, the length scales and power spectra for boundary layers with high freestream turbulence levels, Tu = 20 percent and 12.5 percent, were contrasted with those for boundary layers with low freestream turbulence, Tu = 1 percent.

As shown in Fig. 9(a), the integral scales for velocity fluctuations were much larger for the high turbulence cases throughout the entire boundary layer than for the low freestream turbulence case. Although there was a sharp decrease in the length scales when approaching the wall for the higher turbulence cases, this decrease did not start until well within the boundary layer ($y/\delta < 0.3$).

In Fig. 9(b), which shows the variation of the integral length scales relative to y^+, it is clear that even very near the wall ($y^+ = 15$), the velocity integral length scales for the boundary layers with high freestream turbulence were several times larger than that for a boundary layer with low freestream turbulence. Note that normalizing the integral length scales with the inner length scale, ν/u_τ, or with the distance from the wall, y, still resulted in the length scales for the high freestream turbulence cases being several times larger than for the low freestream turbulence case.

Power spectra for the streamwise velocity component were measured to obtain more detail on the effect of freestream turbulence on turbulence structure near the wall. The spectra, shown in Fig. 10, were measured at the same non-dimensionalized vertical distance from the wall ($y^+ = 15$), for three different turbulence levels (Tu = 1 percent, 12.5 percent, and 20 percent) and are compared to the classical von Kármán's equation for isotropic turbulence. These spectra are normalized using the integral length scale, Λ_f, local mean velocity, U, and the rms

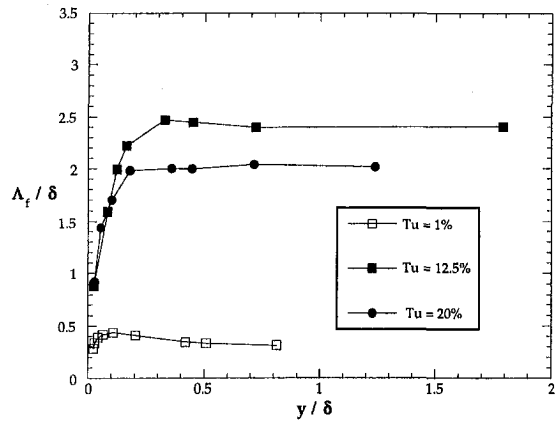

Fig. 9(*a*) Profiles of integral length scales in the boundary layer

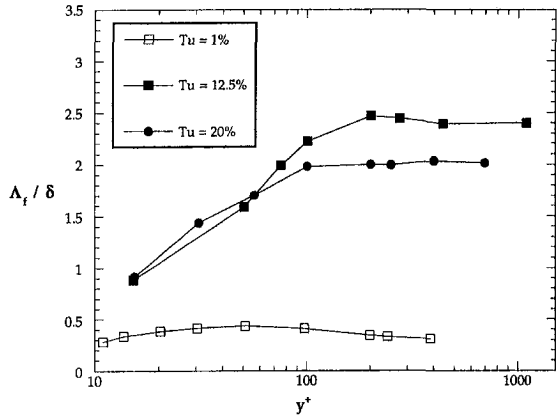

Fig. 9(*b*) Profiles of integral length scales plotted in terms of inner wall variables

velocity, u'. At low wavenumbers $(2\pi f/U)$, the different spectra collapse and agree well with the von Kármán spectrum. The influence of the high freestream turbulence is evident in the larger inertial subrange as compared with the Tu = 1 percent case. However, for the Tu = 12.5 and 20 percent cases, the power spectral density is slightly above the von Kármán equation in the intermediate wavenumber range. The significance of this will be shown in the following discussion.

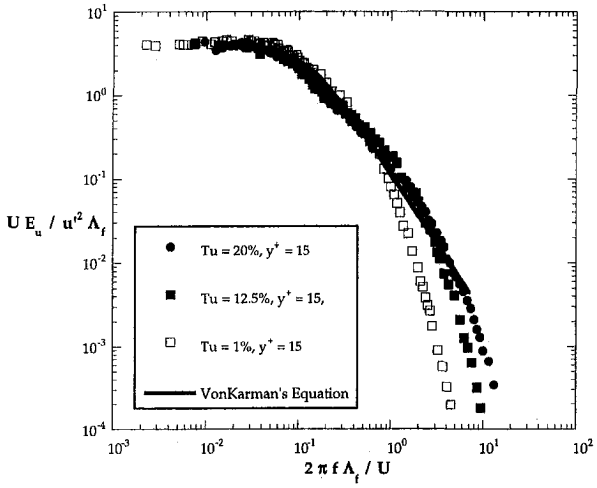

Fig. 10 Comparison of normalized energy density spectra in the boundary layer at a $y^+ = 15$ influenced by freestream turbulence

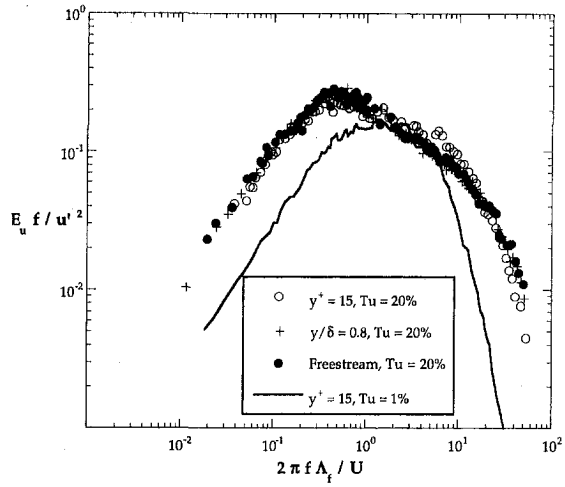

Fig. 11(*a*) Energy spectra as a function of wavenumber normalized by length scale measured throughout the boundary layer influenced by a turbulence level of 20 percent

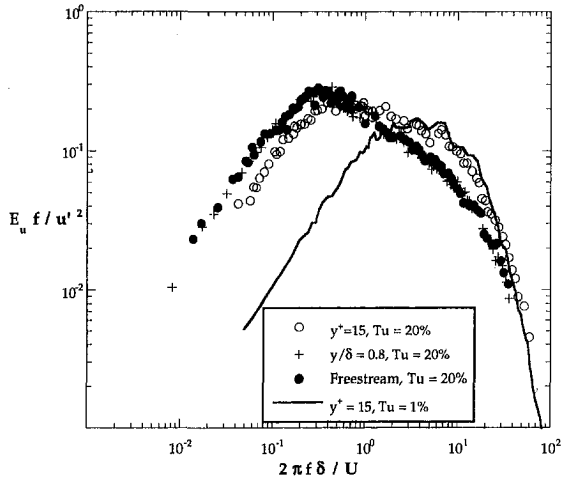

Fig. 11(*b*) Energy spectra as a function of wavenumber normalized by boundary layer thickness measured throughout the boundary layer influenced by a turbulence level of 20 percent

The wavenumber at which the peak power occurs can more easily be seen by plotting the normalized power $(f \cdot E_u/u'^2)$ rather than power density. The influence of the freestream turbulence on the turbulence within the boundary layer was evaluated by comparing freestream power spectra with the power spectra at different positions in the boundary layer, and by comparing with the spectra near the wall for a boundary layer with low freestream turbulence. Figure 11(*a*) shows spectra at three different vertical distances, $y^+ = 15$, $y/\delta = 0.8$ $(y^+ = 440)$, and the freestream for the Tu = 20 percent case. Also, for comparison, the spectrum at $y^+ = 15$ for the Tu = 1 percent case is presented. In Fig. 11(*a*), the wavenumber has been normalized with the local integral scale. From this figure it is clear that there was a much broader frequency range for the highly turbulent case than for the Tu = 1 percent case. Moreover, throughout the entire Tu = 20 percent boundary layer, the power spectra were similar to the freestream power spectrum. This suggests that the freestream turbulence penetrated to $y^+ = 15$, essentially unaffected by the boundary layer turbulence. However, Fig. 11(*a*) shows a slight increase in the Tu = 20 percent power spectrum at wavenumber of about $2\pi f \Lambda_f/U = 10$. The significance of this is illustrated by normalizing the wavenumber with the boundary layer thickness δ, shown in Fig. 11(*b*), rather than the integral length scale, Λ_f. The rational for this is that

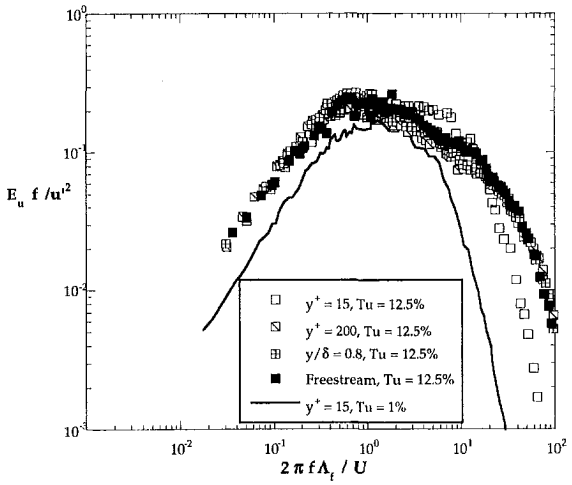

Fig. 12(*a*) Energy spectra as a function of wavenumber normalized by length scale measured throughout the boundary layer influenced by a turbulence level of 12.5 percent

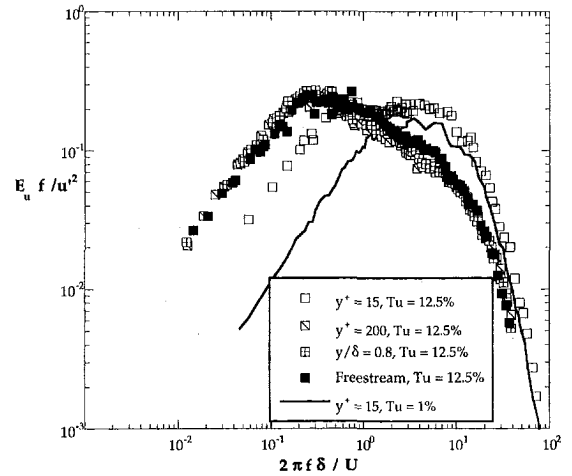

Fig. 12(*b*) Energy spectra as a function of wavenumber normalized by boundary layer thickness measured throughout the boundary layer influenced by a turbulence level of 12.5 percent

the boundary layer generated turbulence will scale with δ, whereas Λ_f is representative of the large scale freestream turbulence because the freestream turbulence dominates the power spectrum. Figure 11(*b*) shows that when normalizing the wavenumber with δ, the spectra at $y^+ = 15$ at low and high freestream turbulence levels correspond well for $2\pi f \delta / U \geq 2$. Consequently, the slight increase in turbulence energy at the higher wavenumbers may be recognized as boundary layer generated turbulence. However, the contribution of the boundary layer generated turbulence energy to the total turbulence energy is still quite small.

A similar analysis was done for turbulence spectra measured in the boundary layer at the position where the freestream turbulence level was Tu = 12.5 percent. Figures 12(*a*) and 12(*b*) show the normalized power spectra case at four different vertical distances, $y^+ = 15$, $y/\delta = 0.33$ ($y^+ = 200$), $y/\delta = 0.8$ ($y^+ = 480$), and the freestream. Also for comparison, the Tu = 1 percent case at a $y^+ = 15$ is presented. There was a similar large broadening of the spectra due to the high freestream turbulence, and at the $y/\delta = 0.33$ and 0.8 locations the power spectra were again essentially the same as the freestream spectrum. However, at a $y^+ = 15$, the power spectrum was double-peaked. Figure 12(*b*) shows that the deviation of the spectrum at higher wavenumbers for the high freestream turbulence case at $y^+ = 15$ corresponded to the Tu = 1 percent case when the wavenumber is normalized with δ. Clearly, at $y^+ = 15$ the turbulence energy at higher wavenumbers is boundary layer generated and is a significant part of the total turbulence energy. However, the low wavenumber freestream turbulence is still a major component of the total turbulence energy.

These results show that at very high freestream turbulence levels, the freestream turbulence significantly affects the turbulence structure very near the wall. Large-scale motions are present throughout the boundary layer as a result of high freestream turbulence levels. Note that the influence of freestream turbulence in increasing the integral length scales and broadening the power spectra was particularly evident in this study because the length scales of the freestream turbulence were significantly larger than the boundary layer generated turbulence. In contrast, Johnson and Johnston (1989) found that freestream turbulence levels as high as Tu = 7.5 percent had no effect on the streamwise velocity spectrum at $y^+ = 15$. Although the lower turbulence level might have been a factor, the relatively small freestream turbulence length scale in their study (essentially equal to the integral scale expected for their boundary layer) probably resulted in spectral characteristics of the freestream turbulence which would be difficult to distinguish from the boundary layer spectra.

Effects of Freestream Turbulence on Boundary Layer Correlation Coefficients

Figure 13 shows the velocity correlation coefficients measured throughout the boundary layer for the highly turbulent flow as compared with the Tu = 1 percent case. For negligible freestream turbulence (Tu = 1 percent), the correlation coefficient measured in the near-wall region is the well-established $R_{uv} = -0.45$. The effect of increasing the freestream turbulence on R_{uv} was quite evident in Fig. 13 which shows a lower magnitude of the correlation coefficient in the outer part of the boundary layer for a Tu = 12.5 percent. However, the correlation coefficient does rise to a magnitude of $R_{uv} = -0.4$ near the wall which is close to the low freestream turbulence value. However, for the freestream turbulence level of Tu = 20 percent, the magnitude of the correlation coefficient is significantly reduced all the way to the wall.

Also shown on Fig. 13 are curves representing the results of Hancock and Bradshaw (1983). In their study, Hancock and Bradshaw concluded that the trends of R_{uv} scaled with the β parameter. Note that our data increase the range of β to $\beta = 3.7$, and that there is a consistent trend of decreasing R_{uv} magnitude with increase in β. The effect of the penetration of uncorrelated, large-scale, freestream turbulence is to reduce the velocity

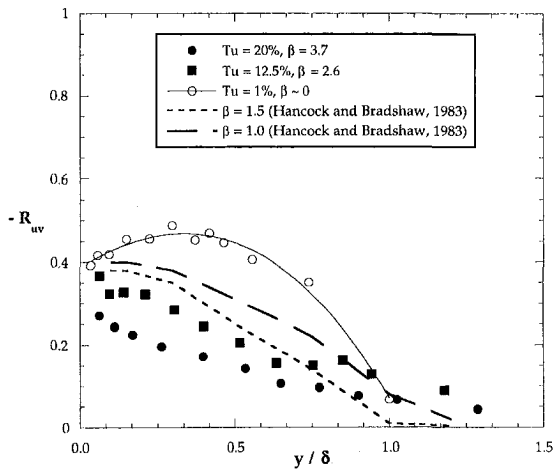

Fig. 13 Effect of freestream turbulence on velocity correlation coefficients

correlation coefficient. These uncorrelated, large-scale freestream eddies have only a small contribution to $\overline{uv}$.

Conclusions

Using a unique freestream turbulence generator, the effect of high freestream turbulence on a two-dimensional, flat plate boundary layer has been studied with high freestream turbulence levels, 10 percent < Tu < 20 percent, significantly higher than most previous investigations. The freestream turbulence was homogeneous and approximately isotropic, and had integral length scales five to eight times larger than that in a boundary layer unaffected by freestream turbulence.

The mean velocity profile was found to retain the log-law profile near the wall for all freestream turbulence levels tested, but the outer region of the profile was significantly altered. Direct measurements of total shear stress (turbulent shear stress and viscous shear stress) verified the validity of the log-law at high freestream turbulence levels. High freestream turbulence caused the outer part of the boundary layer to become much flatter, i.e. the defect velocities in the wake region were substantially reduced, and the wake parameter asymptotically approached a constant value of $\Pi = -0.5$ for large values of the freestream turbulence parameter β.

For low freestream turbulence, the maximum streamwise rms velocity in a boundary layer is $u'/u_\tau = 2.8$. If the freestream u'_∞ level was larger than this, the u' level remained essentially constant at $u' = u'_\infty$ through the boundary layer to within $y^+ = 15$ of the wall. If the freestream u'_∞ level was less than $u'_\infty/u_\tau = 2.8$, then near the wall the u' levels matched the u' levels for a low freestream turbulence boundary layer. For the remainder of the boundary layer the u' levels were approximately constant with $u' = u'_\infty$. In contrast to the u' velocity fluctuations, the v' velocity fluctuations were found to decay significantly as the wall was approached. This decay of v', and the lack of decay for u', were found to correspond closely to predictions of the decay of isotropic turbulence due to wall effects.

Because of the much larger integral length scale of the freestream turbulence compared to the wall generated turbulence, the penetration of freestream turbulence far into the boundary layer was clearly evident from measurements of the integral length scales and the velocity power spectra. For Tu = 20 percent, the velocity power spectrum at $y^+ = 15$ was almost exactly the same as the freestream velocity power spectrum indicating that the freestream turbulence was dominating and essentially unaltered even this close to the wall. For Tu = 12.5 percent, the freestream turbulence still dominated the velocity power spectrum at $y^+ = 15$, but there was a distinct contribution from wall generated turbulence at higher wavenumbers. In all high freestream turbulence cases, the velocity power spectra were much broader than for the low freestream turbulence boundary layer because of the much larger length scales for the freestream turbulence.

Another effect of the dominance of freestream turbulence within the boundary layer was the reduction of R_{uv} correlation coefficient throughout the boundary layer. The reduced values of R_{uv} were because of the uncorrelated nature of the freestream turbulence.

As a final note, we point out that these results should not be interpreted in terms of the freestream turbulence levels alone, but rather the combination of the freestream turbulence levels and the large turbulence length scale. The decay of normal velocity fluctuation near the wall, and characteristics of the velocity power spectra were clearly dependent on the length scale of the turbulence. Furthermore, the strong penetration of the turbulence into the boundary layer, and the dominance of the freestream turbulence within the boundary layer may well not have occurred if the length scale of the freestream turbulence had been of the same order or smaller than the length scale of the wall generated turbulence.

Acknowledgments

The authors would like to thank both Wright Laboratory and Allied-Signal for their support of this project.

References

Ames, F. E., and Moffat, R. J., 1990, "Heat Transfer with High Intensity, Large Scale Turbulence: The Flat Plate Turbulent Boundary Layer and the Cylindrical Stagnation Point," Stanford University Report HMT-44.

Blair, M. F., 1983, "Influence of Free-Stream Turbulence on Turbulent Boundary Layer Heat Transfer and Mean Profile Development: Part II-Analysis of Results," ASME *Journal of Heat Transfer,* Vol. 105, pp. 41–47.

Bradshaw, P., 1978, *Topics in Applied Physics, Turbulence,* P. Bradshaw, ed., Vol. 12, 2nd ed., New York, Springer-Verlag.

Charnay, G., Mathieu, J., and Comte-Bellot, G., 1976, "Response of a Turbulent Boundary Layer to Random Fluctuations in the External Stream," *Physics of Fluids,* Vol. 19, pp. 1261–1272.

Comte-Bellot, G., "Simple Eulerian Time Correlation of Full- and Narrow-Band Velocity Signals in Grid-Generated, 'Isotropic' Turbulence," *Journal of Fluid Mechanics,* Vol. 48, part 2, pp. 273–337.

Edwards, R. V., 1987, "Report on the Special Panel on Statistical Particle Bias Problems in Laser Anemometry," ASME JOURNAL OF FLUIDS ENGINEERING, Vol. 109, pp. 89–93.

Gad-el-Hak, M., and Bandyopadhyay, P. R., 1994, "Reynolds number effects in wall-bounded turbulent flows," *Applied Mechanical Review* Vol. 47, No. 8, pp. 307–365.

Hancock, P. E., and Bradshaw, P., 1983, "The Effect of Free-stream Turbulence on Turbulent Boundary Layers," ASME JOURNAL OF FLUIDS ENGINEERING, Vol. 105, pp. 284–289.

Hancock, P. E., and Bradshaw, P., 1989, "Turbulence Structure of a Boundary Layer Beneath a Turbulent Freestream," *Journal of Fluid Mechanics,* Vol. 205, pp. 45–76.

Hinze, J. O., 1975, *Turbulence,* 2nd Edition, New York, McGraw-Hill.

Hoffmann, J. A., and Mohammadi, K., 1991, "Velocity Profiles for Turbulent Boundary Layers Under Freestream Turbulence," ASME JOURNAL OF FLUIDS ENGINEERING, Vol. 113, pp. 399–404.

Hunt, J. C. R., and Graham, J. M. R., 1978, "Free-stream turbulence near plane boundaries," *Journal of Fluid Mech.* Vol. 84, pp. 209–235.

Johnson, P. L., and Johnston, J. P., 1989, "Active and Inactive Motions in a Turbulent Boundary Layer—Interactions with Free-Stream Turbulence," *Proceedings 7th Symposium of Turbulent Shear Flows,* Stanford University, pp. 20.2.1–20.2.6.

Kestin, J., 1966, "The Effect of Freestream Turbulence on Heat Transfer Rates," *Advances in Heat Transfer,* Vol. 3., New York, Academic Press.

Maciejewski, P. K., ands Moffat, R. J., 1992, "Heat Transfer with Very High Free Stream Turbulence: Part II-Analysis of Results," ASME *Journal of Heat Transfer*, Vol. 114, pp. 834–839.

Simonich, J. C., and Bradshaw, P., 1978, "Effect of Free-Stream Turbulence on Heat Transfer through a Turbulent Boundary Layer," ASME *Journal of Heat Transfer,* Vol. 100, pp. 671–677.

Thole, K. A., and Bogard, D. G., 1994, "Enhanced Heat Transfer and Shear Stress due to High Freestream Turbulence," ASME *Journal of Turbomachinery,* Vol. 117, no. 5, pp. 418–424.

Thole, K. A., Bogard, D. G., and Whan-Tong, J. L., 1994, "Generating High Freestream Turbulence Levels," *Experiments in Fluids* Vol. 17, pp. 375–380.

Thomas, N. H., and Hancock, P. E., 1977, "Grid Turbulence Near a Moving Wall," *Journal of Fluid Mechanics,* Vol. 82, pp. 481–496.

Townsend, A. A., 1956, *The Structure of Turbulent Shear Flow,* Cambridge Press.